Supplemental Data

Novel Evolutionary-Conserved Role for the ADNP Protein Family that is Important for Erythropoiesis

Efrat Dresner, Anna Malishkevich, Carmit Arviv, Shelly Leibman Barak, Shahar Alon, Rivka Ofir, Yoav Gothilf and Illana Gozes

List of Supplemental Items:

1. Supplemental Experimental Procedures
2. Supplemental Tables S1-S2
3. Supplemental Figures S1-S10
4. Legends and still images for supplemental Movies S1-S6
5. Supplemental References

Supplemental Experimental Procedures

O-dianisidine staining

Hemoglobin activity was detected in whole embryos by performing o-dianisidine staining as described (1). Briefly, embryos were dechorionated and stained for 15 minutes in the dark in 0.6 mg/ml o-dianisidine (Sigma, St. Louis, MO, USA), 0.01M sodium acetate (pH 4.5), 0.65% H_2O_2 and 40% (v/v) ethanol. Embryos were post-fixed in 4% paraformaldehyde for at least 1hr at 4^0C and stored in 70% glycerol for microscopy. The basis of this assay is that hemoglobin catalyzes the H_2O_2 mediated oxidation of o-dianisidine, producing a dark red stain in hemoglobin-positive cells.

Whole-mount in situ hybridization (WMISH)

WMISH was carried out according to established protocol (2,3) with a few modifications. Briefly, embryos were treated with 100% acetone for 8 min at −20 °C, rehydrated through a graded series of methanol concentrations, treated with proteinase K (10 µg/ml, Roche Applied Science, Penzberg, Germany) for 0-40 min (depending on the developmental stage of the embryos), fixed again for 30 min, washed in PBS and pre-hybridized for 4hrs at 65°C in hybridization buffer [50% formamide, 5 × standard sodium citrate (SSC, Sigma), 5mM EDTA, 0.1% Tween-20, 0.1% CHAPS (Roche), 50 µg/ml heparin (Sigma) and 1 mg/ml yeast RNA]. Hybridization was carried out overnight (1ng/µl probe in hybridization buffer, 65^0C). Embryos were then washed twice with 50% formamide, 1 × SSC and 0.15% CHAPS at 65°C for 30 min, once with 2 × SSC and 0.3% CHAPS at 65°C for 15 min and twice with 0.2 × SSC and 0.3% CHAPS at 65°C for 30 min. After 1 hour pre-incubation in blocking solution [2% blocking reagent (Roche) and 5% calf serum in MAB buffer (0.1M maleic acid, 150mM NaCl, pH 7.5)], anti-DIG antibody conjugated to alkaline phosphatase (AP, Roche, 1:5000, diluted in

blocking solution) was applied to the embryos for 3hrs. The riboprobe-antibody complex was detected by the enzymatic reaction of AP with the chromogenic substrate BM purple (Roche). Staining reaction was stopped by replacing BM purple substrate with PBS followed by fixation in 4% paraformaldehyde. Fixed embryos were placed in 70% glycerol for observation and photography using a dissecting stereoscope (SZX12, Olympus) equipped with digital camera (DP70, Olympus). In each experiment, embryos hybridized with the same probe were stained under the same conditions and for the same time period using identical microscopic and camera settings.

RNA interference and transfections

For mouse ADNP silencing, two shRNA clones (Sigma) were used in order to show specificity. All constructs were in a pLKO.1-puro vector. The sequences used are: (I) sh68, 5'-CCGGGCCTACAGATACCCTACTCAACTCGAGTTGAGTAGGGTATCTGTAGGCTTTTTG-3'; (II) sh71, 5'-CCGGGATTCTTATGAGGCTAGGAAACTCGAGTTTCCTAGCCTCATAAGAATC TTTTTG-3'.

For mouse ADNP2 silencing, a mixture of two stealth small interfering RNA (siRNA) duplexes (Invitrogen, Carlsbad, CA, USA) was used: (I) sense, 5'-GGAGAUGUUUCUCCUUGGGAACCUU-3'; (II) sense, 5'-GGAAAGAAAGCGAGAUACCGGACAA-3'. A mixture of two scrambled stealth siRNA duplexes was used as a control: (I) sense, 5'-GGAGUUUCUCUUCGUGGAACAGCUU-3'; (II) sense, 5'-GGAAAGCGAGAGAUAGCCAGAACAA-3'.

For mouse ADNP knockdown, 1×10^5 MEL cells were plated in 500µl growth medium without antibiotics on 24 well plate and transfected with 1µg of shRNA plasmid. 6hrs after transfection, 2% DMSO was added to the cells. For ADNP2 silencing, 5×10^4 MEL cells were plated in 100µl growth

medium without antibiotics on 24 well plate and immediately transfected with a 50pmol mixture of two siRNA duplexes. 6hrs later, 400µl of fresh medium supplemented with 2% DMSO was added.

For MEL growth curves analyses and protein extraction, cells were plated on 6-well culture plates, and the number of cells and transfection conditions were adjusted to the dish surface area. Viable cells were counted daily following Trypan-blue (Sigma) staining.

RNA extraction

Total RNA was extracted from MEL cells by the RNeasy Plus Mini Kit (Qiagen, Hilden, Germany). RNA integrity was determined by fractionation on 1% agarose gel and staining with ethidium bromide. RNA quantity (OD260) was determined by NanoDrop spectrophotometer (NanoDrop Technologies, Wilmington, DE, USA).

Reverse transcription and quantitative real time PCR

Samples with the same amount of total RNA were used to synthesize single-strand cDNA employing the Applied Biosystems High Capacity cDNA Reverse Transcription Kit (Applied Biosystems, Foster City, CA, USA) and random hexamers primers as before.(4) Primer pairs (supplemental Table 2) were designed using the primer3 web interface (http://frodo.wi.mit.edu/primer3/) and synthesized by Sigma-Genosys (The Woodlands, TX, USA). To avoid amplification of contaminating genomic DNA, primers were designed to exon-exon junctions. Real-time PCR was performed using the SYBR® Green PCR Master Mix and ABI PRISM 7900 Sequence Detection System instrument and software (Applied Biosystems) as previously described (4). *18S* ribosomal RNA was used as the normalization control gene. Product specificity was confirmed in the initial experiments by agarose gel electrophoresis and sequencing and routinely by melting curve analysis.

Protein extraction and western blot analysis

Total protein extraction from MEL cells was performed using RIPA buffer (50mM Tris pH 7.5, 150mM NaCl, 1% NP-40, 0.1% SDS and 0.5% deoxycholic acid) supplemented with protease inhibitors cocktail (Sigma) and 5 mM EDTA (ethylenediaminetetraacetic acid). Proteins were quantified using BCA^{TM} Protein Assay Kit (Pierce, Rockford, IL, USA). ~10 µg protein extract per lane was separated by electrophoresis on a 10% (w/v) polyacrylamide gel containing 0.1% SDS (SDS-PAGE). Molecular weights were determined using Precision Plus Protein Standards (Dual Color, BioRad, Hercules, CA, USA). Following electrophoresis, proteins were transferred to nitrocellulose membrane (Whatman Plc., Kent, UK) and nonspecific antigen sites were blocked with 5% nonfat dried milk (w/v) in TBST (10mM Tris pH 8, 150mM NaCl and 0.05% Tween 20). Antigen detection was performed over-night at 4^0C using mouse monoclonal anti-ADNP (1:400, BD Biosciences, San Jose, CA, USA), rabbit anti-*Brg1* antibody (1:5000, Sigma) and mouse monoclonal anti-α-tubulin (1:1000, clone DM1A, Sigma) as an internal standard. Antibody–antigen complexes were detected using horseradish peroxidase (HRP)-conjugated goat anti-mouse or anti-rabbit IgG secondary antibodies (Jackson ImmunoResearch, West Grove, PA, USA) and visualized by chemiluminescent kit (Pierce). Densitometric measurements were performed using the Tina 2.10g Software (Ray Test, Straubenhardt, Germany).

Table S1: Splicing MO's Oligos for Zebrafish *adnp1* and *adnp2* Genes

MO Name	***adnp1a*-sp$_1$MO**	***adnp1a*-sp$_2$MO**	***adnp1b*-spMO**
Sequence	5'-TAGTCCTGCAACA TTTGAGAAACCA-3'	5'-CACTGTTCAAAA GCAATCACCTCCA-3'	5'-AAGTGTAATATCT ACTCACATCAAC-3'
Target	Intron3-exon4 boundary	Exon2-intron2 boundary	Exon2-intron2 boundary
Presumed function	Inclusion of intron3	Exclusion of axon2 which contains the first ATG codon, necessary for translation initiation	Exclusion of axon2 which contains the first ATG codon, necessary for translation initiation
Was the expected phenotype observed?	**Yes**	No	No
RT-PCR	An additional higher band representing the inclusion of intron 3 was found in MO-injected embryos	An additional lower band representing the exclusion of exon2 in MO-injected embryos (supplemental Figure S1)	An additional lower band representing the exclusion of exon2 in MO-injected embryos (supplemental Figure S1)
Sequencing	Incorporation of intron 3 into the *adnp1a* transcript. Notably 10 base-pairs (bp) were deleted from a repetitive region in the center of the intron. However, this appears to be an artifact of the RT-PCR reaction, resulting from homology-dependent template switching (5)	Deletion of exon2	Only 45 nucleotides at the end of the exon2 were omitted. The beginning of the exon, including the ATG codon, were not affected
Remarks	Inclusion of intron 3 is predicted to cause a truncation of the *adnp1a* protein (134 amino acid protein instead of the predicted 969 amino acid protein).	Exon4 contains 18 ATG codons located on the same reading-frame of the predicted protein. As exon4 is the largest exon in the *adnp1a* gene, containing most of the functional domains, it is possible that translation was initiated at another ATG, producing functional protein of 26-840 amino acid (depending on the ATG selected), instead of the predicted 969 amino acid	Exclusion of 45 nucleotides is predicted to cause a deletion of 15 amino acid (988 amino acid protein instead of the predicted 1003 amino acid protein) without changing the reading-frame

		protein. Several of these ATG codons are consistent with the Kozak consensus sequence (6)	

MO Name	***adnp2a*-sp$_1$MO**	***adnp2a*-sp$_2$MO**	***adnp2b*-spMO**
Sequence	5'-GATACTGAGAAA GGAAGGCAACATC-3'	5'-CAGATCTACAG TACTCTACCTCCAG-3'	5'-TTCCCACTGAG GATGGAAAATTCTT-3'
Target	Intron3-exon4 boundary	Exon2-intron2 boundary	Intron3-exon4 boundary
Presumed MO function	Inclusion of intron3	Exclusion of axon2 which contains the first ATG codon, necessary for translation initiation	Inclusion of intron3
Was the expected phenotype observed?	No	No	**Yes**
RT-PCR	No change in the *adnp2a* transcript between MO-injected and wild-type embryos (supplemental Figure S1)	An additional lower band representing the exclusion of exon2 in MO-injected embryos (supplemental Figure S1)	An additional lower band in MO-injected embryos (supplemental Figure S1)
Sequencing	No change in the *adnp2a* transcript between MO-injected and wild-type embryos	Deletion of exon2	Deletion of 53 nucleotides at the beginning of exon4
Remarks		Exon4 contains 26 ATG codons located on the same reading-frame of the predicted protein. As exon4 is the largest exon in the *adnp2a* gene, containing most of the functional domains, it is possible that translation was initiated at another ATG, producing functional protein of 96-854 amino acid (depending on the ATG selected), instead of the predicted 962 amino acid protein. Several of these ATG codons are consistent with the Kozak consensus	Such a deletion is predicted to cause a truncation of the *adnp2b* protein (81 amino acid protein instead of the predicted 947 amino acid protein)

		sequence (6)	

Table S1. Splicing MO's oligos tested for zebrafish *adnp1* and *adnp2* genes. To validate our previous results, 6 splicing MO's (spMO's) were designed. It should be mentioned that translation-blocking MO's were our initial choice, as our expression profile analyses indicated that all four zebrafish genes are maternally expressed (supplemental Figure 3C). A translation MO (tMO), while not affecting RNA levels, has the advantage of blocking maternal gene expression, in contrast to a splicing-blocking MO (spMO) (7). Thus, the efficacy of gene knockdown achieved by tMO can be only quantified by western blot analysis using appropriate antibodies and not by RT-PCR. Since antibodies against zebrafish ADNP proteins are not available and the mammalian ADNP antibody does not recognize the zebrafish protein (data not shown), we were not able to demonstrate the correlation between phenotypes and the extent of knockdown. To overcome this obstacle, 6 spMO's were tested for each one of zebrafish ADNP and ADNP2 orthologues. Two of these spMO's, *adnp1a*-sp_1MO and *adnp2b*-spMO, resulted in non-functional mRNA transcripts and have consequently shown the expected phenotype, while the others failed to do so, probably because they did not cause the appearance of defective transcripts. Interestingly, 2 MO's oligos caused complete deletion of exon2 that contains the first ATG codon, however failed to produce the expected phenotype. This might indicate that 1] exon2 is not necessarily required for protein activity and 2] several downstream ATGs might function as translation initiation sites.

Table S2. Reverse Transcription and Quantitative real-time PCR: Primer Pairs

Primer	Sequence
Mouse ADNP (NM_009628)	5'- acgaaaaatcaggactatcgg -3' 5'- ggacattccggaaatgacttt -3'
Mouse ADNP2 (NM_175028)	5'- ggaaagaaagcgagataccg -3' 5'- tcctggtcagcctcatcttc -3'
Mouse *β-globin* (Hbb-b1) (NM_008220)	5'- gcaggctgctggttgtct-3' 5'- catgggccttcactttgg-3'
Mouse *band3* (Slc4a1) (NM_011403)	5'- tgcttgtgggactgtccat -3' 5'- aagagctggatgccactgag -3'
Mouse *c-kit* (NM_001122733)	5'- caaaggaaatgcacgactgc-3' 5'- tcccataggaccagacatca-3'
Mouse *18S* ribosomal RNA (NR_003278)	5'- cctgcggcttaatttgactc-3' 5'- aactaagaacggccatgcac-3'

Supplemental Figures

Figure S1.

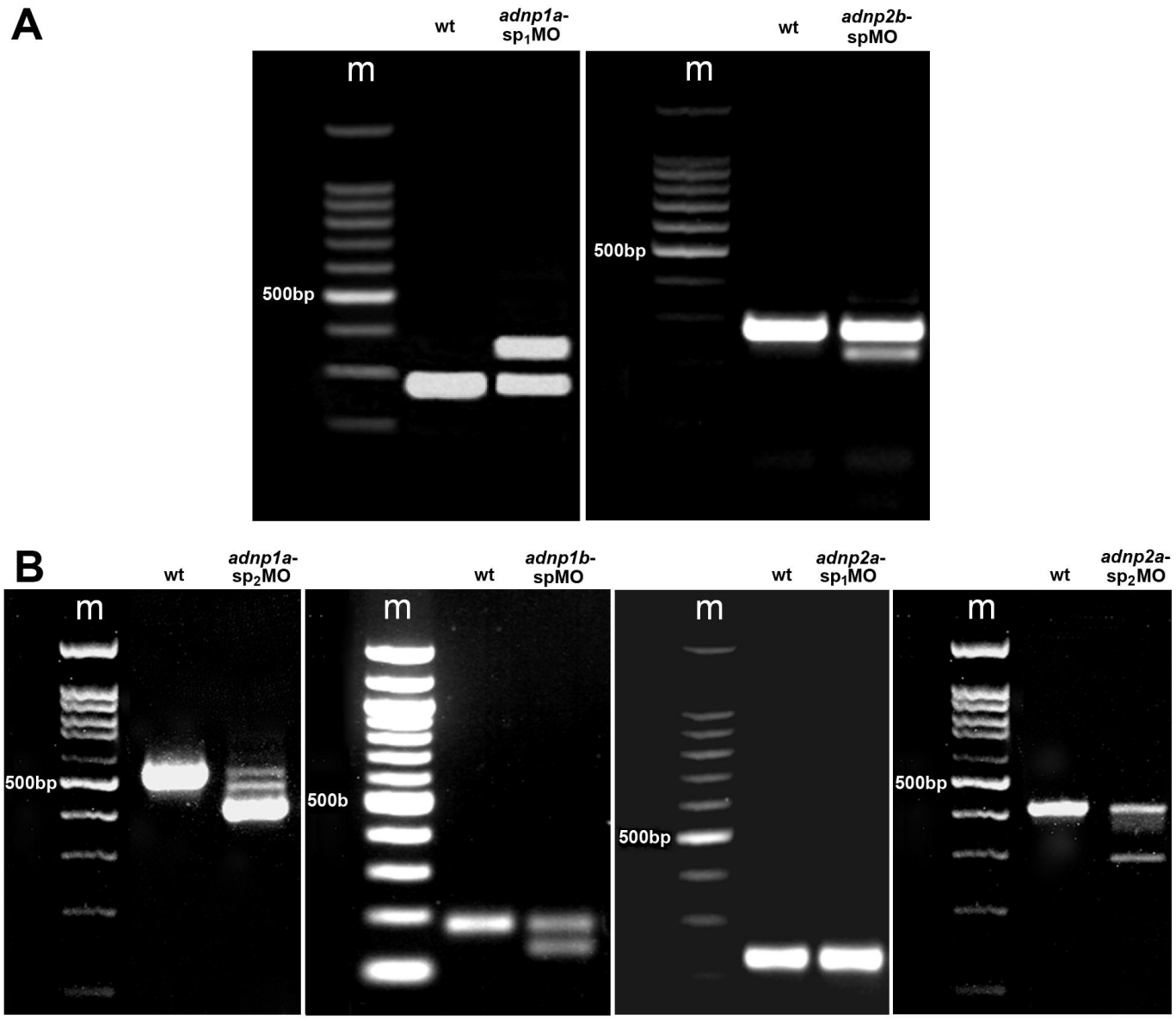

Figure S1. RT-PCR analyses of *adnp1* and *adnp2* sp-MO's oligos. MO-injected and un-injected embryos were sampled (~20 embryos/sample) at 24 hpf. Total RNA was extracted (EZ-RNA Total RNA Isolation Kit, Biological Industries, Beit Haemek, Israel), treated by DNase (DNA-free kit, Ambion, Austin, TX, USA) and reversed-transcribed using High Capacity cDNA Reverse

Transcription Kit (Applied Biosystems). PCR amplification was performed using set of primers flanking the presumed MO target. PCR products were separated on an agarose gel, cut from the gel and sequenced. (A) *adnp1a*-sp$_1$MO and *adnp2b*-spMO injection alters *adnp1a* and *adnp2b* splicing as shown by RT-PCR analysis and have consequently shown the expected phenotype as described in the main article. An additional higher band representing the inclusion of intron3 and an additional lower band representing exon4 deletion was found in *adnp1a*-sp$_1$MO and *adnp2b*-spMO injected embryos, respectively. Detailed sequence analysis is found in supplemental table 1. (B) RT-PCR analyses of *adnp1a*-sp$_2$MO, *adnp1b*-spMO, *adnp2a*-sp$_1$MO and *adnp2a*-sp$_2$MO. Detailed explanations including RT-PCR and sequence analyses are in supplemental table S1.

Figure S2.


Alignment of adnp1a-sp1MO target sequence with the three other ADNPs genes
adnp1a 1 tggtttctcaaatgttgcaggacta 25
adnp1b 835 tggt-----aaatgttgcatg-cta 853
adnp1a 3 gtttc------tcaa-------atgttgcag--gacta 25
adnp2a 2149 gtttccactgatcaatcttgagatgtttcagcagccta 2186
adnp1a 1 tggtttct---caaat---------gttg----cag 20
adnp2b 2302 tggtttctatagaaattgtatataggttggtgtcag 2337
Alignment of adnp1b-tMO target sequence with the three other ADNPs genes
adnp1b 3 atgtttcaactcccagtgaacaa 25
adnp1a 356 atgtttcagcttccagtgaataa 378
adnp1b 2 aatgtttcaactcccagtgaacaa 25
adnp2a 260 aatgtatcagattccagtgaagaa 283
adnp1b 1 gaa--tgtttcaac----------tcccagt----------gaacaa 25
adnp2b 178 gaaagtgttgcaccatgtaccagtttccagtaaaaggtttggagaagatccgcagaacaa 237
Alignment of adnp2a-tMO target sequence with the three other ADNPs genes
adnp2a 2 agca----aaatgtatcagattccagtg 25
adnp1a 346 agcagaagagatgtttcagcttccagtg 373
adnp2a 2 agcaaaatgtatcagattccagtg 25
adnp1b 351 agaagaatgtttcaactcccagtg 374
adnp2a 3 gcaaaatgtatcagattccagt 24
adnp2b 187 gcaccatgtaccagtttccagt 208
Alignment of adnp2b-tMO target sequence with the three other ADNPs genes
adnp2b 2 atgtaccagtttccagtaaa 21
adnp1a 356 atgtttcagcttccagtgaa 375
adnp2b 2 atgtaccagtttccagtaaa 21
adnp1b 357 atgtttcaactcccagtgaa 376
adnp2b 2 atgtaccagtttccagtaaa 21
adnp2a 261 atgtatcagattccagtgaa 280

Figure S2. Alignment of *adnp1* and *adnp2* morpholinos (MO's) target sequences with the three other *adnp1/adnp2* genes. BLAST analysis was performed to verify that the MO's were not predicted to bind gene sequences other than their targets, and that their target sequence was not conserved among the other zebrafish *adnp1/adnp2* genes to preclude off-target binding. The target sequence of each one of the MO's oligos was aligned with the three other *adnp1/adnp2* genes using the EMBOSS Pairwise Alignment Algorithm to preclude MO's mistargeting. The sequence design results in at least 5 mismatched nucleotides dispersed along a 25mer MO (20% mismatch), when comparing each MO target with the three other family member genes.

Figure S3.

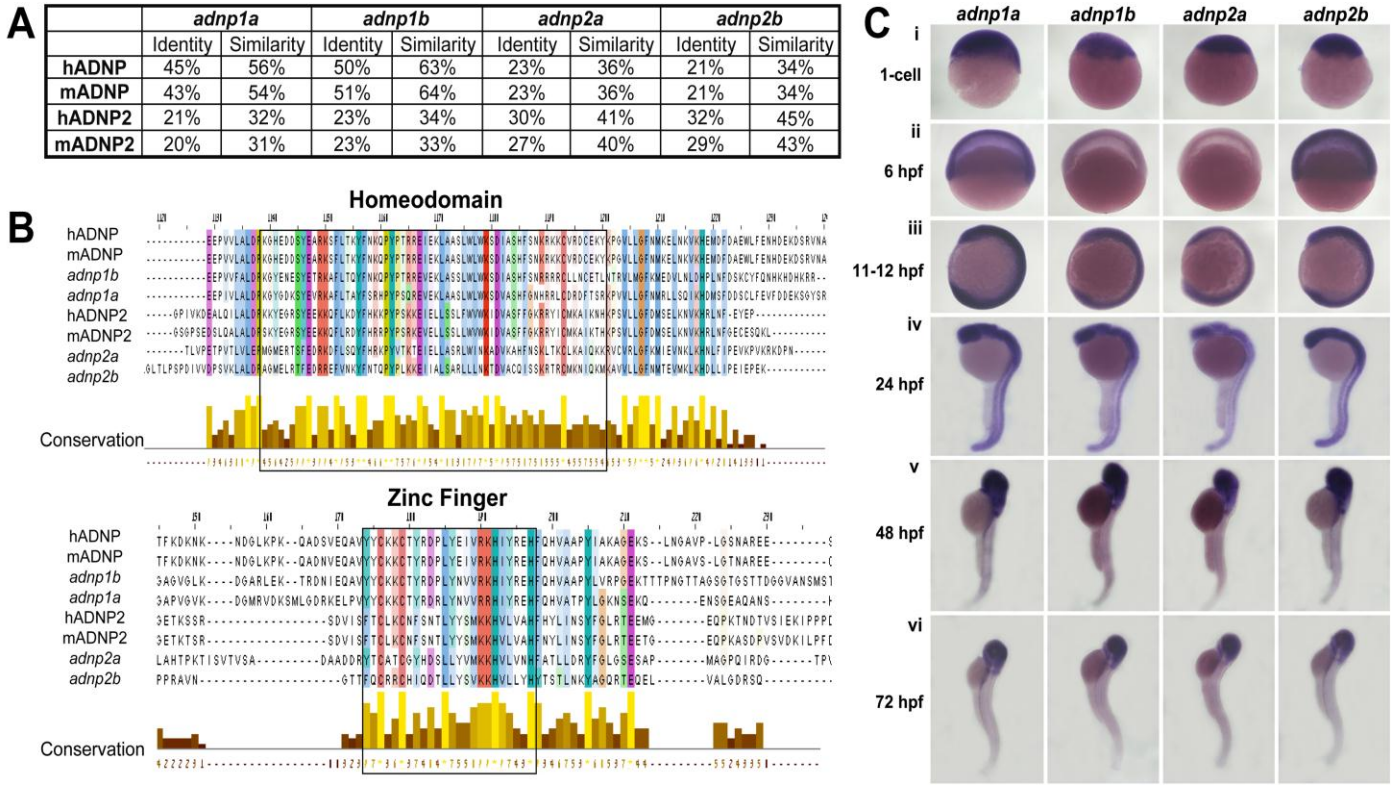

	adnp1a		adnp1b		adnp2a		adnp2b	
	Identity	Similarity	Identity	Similarity	Identity	Similarity	Identity	Similarity
hADNP	45%	56%	50%	63%	23%	36%	21%	34%
mADNP	43%	54%	51%	64%	23%	36%	21%	34%
hADNP2	21%	32%	23%	34%	30%	41%	32%	45%
mADNP2	20%	31%	23%	33%	27%	40%	29%	43%

Figure S3. Identification and expression profile of ADNP and ADNP2 zebrafish orthologues. BLAST search for human ADNP (NP_056154) and ADNP2 (NP_055728*)* orthologues in zebrafish

revealed two zebrafish orthologues for each mammalian gene. *adnp1a* (NP_001073484) and *adnp1b* (XP_002666520) are the two mammalian ADNP orthologues, while *adnp2a* (NP_001091735) and *adnp2b* (NP_001073482) are the two mammalian ADNP2 orthologues. The existence of two zebrafish orthologues for each mammalian gene reflects partial genome duplication that occurred during early evolution of teleosts (8). (A) Amino acid identity and similarity between zebrafish, mouse and human ADNP and ADNP2 (%). (B) Multiple sequence alignment of ADNP and ADNP2 in zebrafish, mouse and human. High conservation levels were found, especially along the homeodomain and zinc-fingers motifs which exist in all four zebrafish orthologues. Two representative highly conserved regions are shown: the homeodomain (top) and one of the zinc-finger domains (below, note the high conservation, especially along the two cysteines and two histidines which are the functional residues of this domain). (C) Expression profile of zebrafish *adnp1* and *adnp2* during embryonic development by WMISH on embryos from 1-cell to 72 hours-post-fertilization (hpf). All zebrafish *adnp1* and *adnp2* transcripts were detected at the 1-cell stage, prior to the onset of zygotic expression which starts at ~2.75 hpf (9), and are therefore maternally deposited. While expression of *adnp1a* and *adnp2b* was detected during all stages of embryonic development examined, the expression of *adnp1b* and *adnp2a* was detected at the 1-cell stage, before the onset of zygotic expression, then, during gastrulation, at 6 hpf, no signal was detected, and at 11-12 hpf (segmentation) signal was detected again and was visible until 72 hpf. This pattern indicates that all four transcripts are maternally expressed, but later on, zygotic expression of *adnp1a* and *adnp2b* precedes that of *adnp1b* and *adnp2a*. In addition, at early developmental stages, *adnp1* and *adnp2* were ubiquitously expressed throughout the embryos, but as development progressed, expression was highest at the anterior region of the embryos. (i-ii) are side views, (iii-vi) are lateral views with anterior to the top and ventral to the left. N≥15 embryos/staining.

Figure S4.

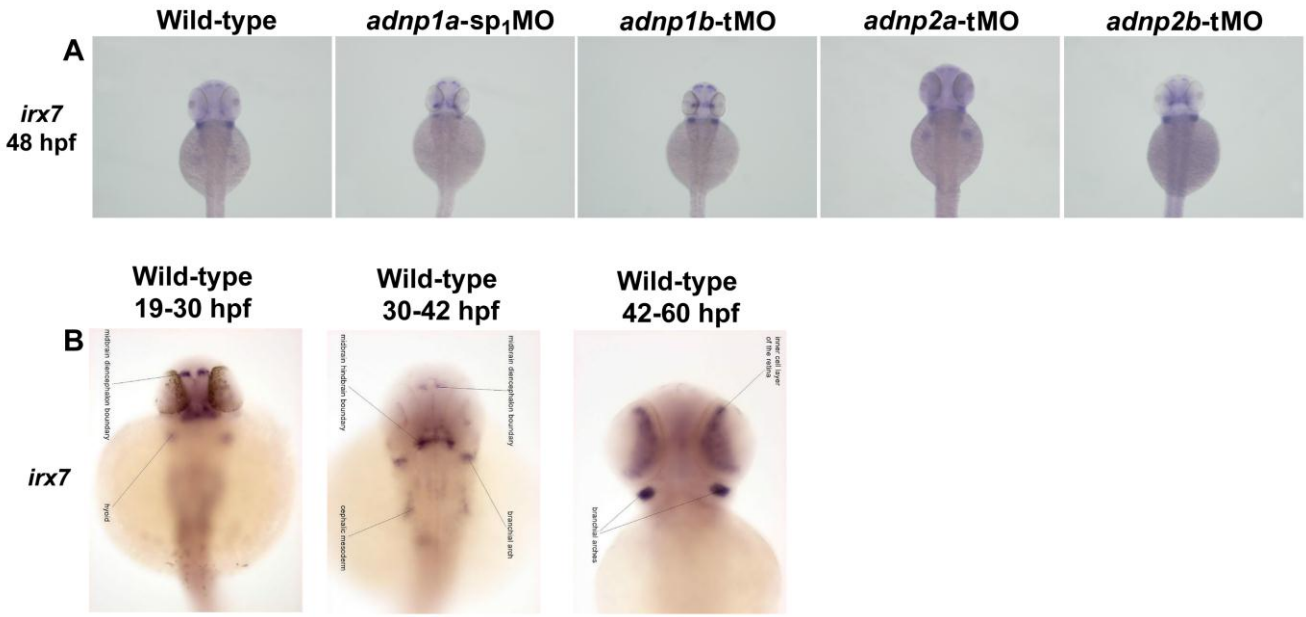

Figure S4. *adnp1* knockdown embryos suffer from developmental delay. (A) Preliminary data showing the expression pattern of *irx7* (10) [CNS marker] at 48 hpf in *adnp1* and *adnp2* MO's-injected embryos. Embryos are in dorsal view, with anterior to the top. (B) *irx7* expression pattern in wild-type embryos from 19-60 hpf. Pictures are taken from the ZFIN database (http://zfin.org). Note that while *irx7* expression pattern in *adnp2a*-tMO, *adnp2b*-tMO and wild-type embryos at 48 hpf (A) resembles that of wild-type embryos at the same developmental stage (42-60 hpf), the expression pattern in *adnp1a*-sp$_1$MO and *adnp1b*-tMO injected embryos at 48 hpf resembles that of younger embryos at around 19-30 hpf.

Figure S5.

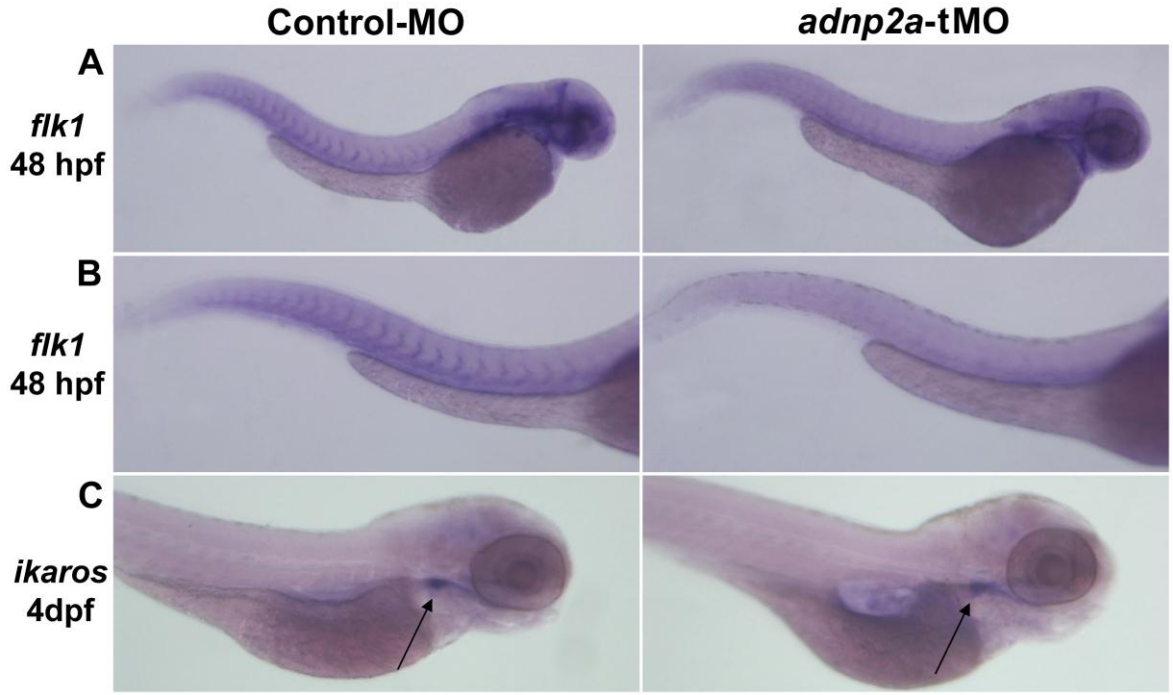

Figure S5. *adnp2a* silencing has no effect on definitive hematopoiesis markers or gross heart morphology, but negatively affects vasculogenesis. (A-B) Expression of the VEGF receptor, *flk1*, blood vessel marker (11) was reduced in *adnp2a*-tMO injected embryos at 48 hpf (76% of embryos, n=17 versus 0% of embryos, n=17 for control-MO), suggesting impaired blood vessel formation. (C) *ikaros*, marker of the lymphoid population (12) that differentiates only in the definitive wave of hematopoiesis, was normally expressed at the thymus (arrows) of 4 dpf *adnp2a*-tMO injected embryos (100% of embryos, n=18). Expression of *c-myb* (11), additional definitive marker, was also normal in 30-36 hpf *adnp2a*-tMO injected embryos (data not shown, 100% of embryos, n=20). Additional preliminary results indicated normal gross heart development, as the expression of the pan-cardiac marker *cmlc2* (13) appeared normal in the knockdown embryos (data not shown). Embryos are at lateral view, anterior to the right. A and B are 48 hpf embryos, C is 4 dpf embryo. N≥15 embryos/staining.

Figure S6.

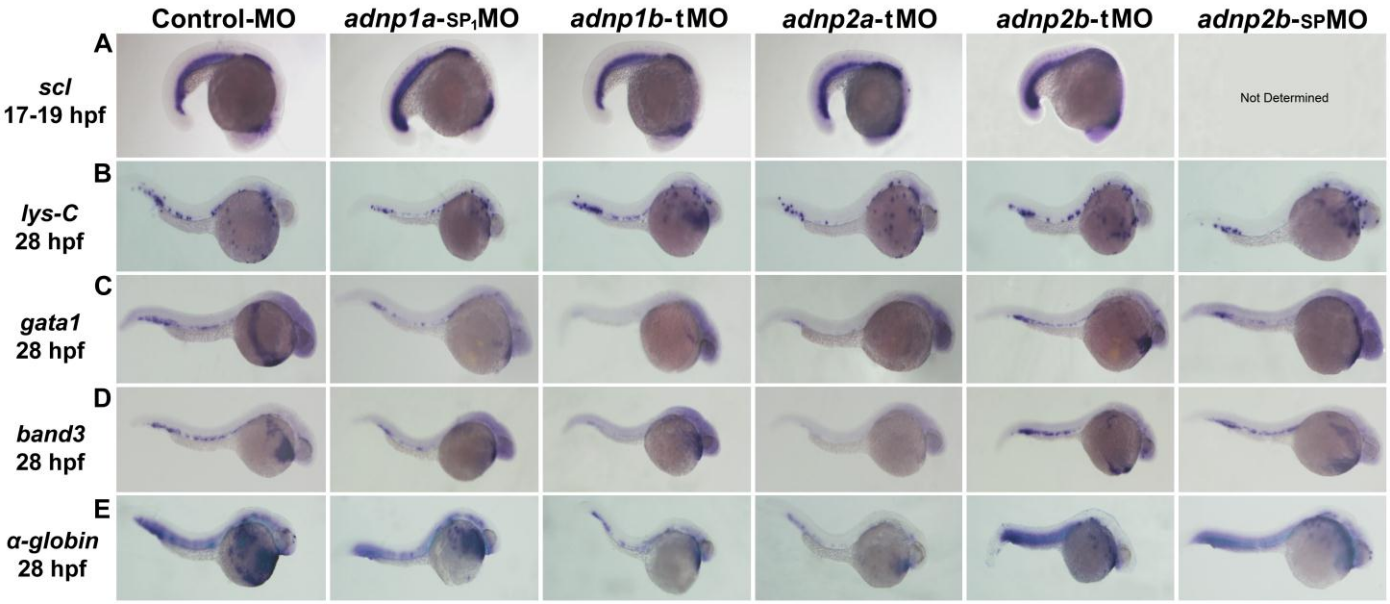

Figure S6. Silencing of *adnp1a, adnp1b* and *adnp2b* results in impaired maturation of the erythroid lineage, similar to the *adnp2a* knocdown phenotype. Expression of *scl* at 17-19 hpf (A) and of *lys-C* (B), *gata1* (C), *band3* (D) and embryonic *α-globin1* (E) at 28 hpf was evaluated for *adnp1a*-sp$_1$MO, *adnp1b*-tMO, *adnp2b*-tMO and *adnp2b*-spMO. Results indicate normal specification of mesoderm into the hematopoietic lineage (A) and normal myeloid development (B), but impaired maturation and differentiation of the erythroid lineage (C-E). A-E are lateral views with anterior to the bottom (A) or to the right (B-E). [Summary of staining results: *scl* 17-19 hpf: 100% of embryos, n=11 for *adnp1a*- sp$_1$MO, *adnp1b*-tMO and *adnp2b*-tMO. *lys-C* 28 hpf: 94% of embryos, n=18 for *adnp1a*-sp$_1$MO, 92% of embryos, n=13 for *adnp1b*-tMO, 100% of embryos, n=26 for *adnp2b*-tMO and 78% of embryos, n=9 for *adnp2b*-spMP. *gata1* 28hpf: 96% of embryos, n=25 for *adnp1a*-sp$_1$MO, 92% of embryos, n=13 for *adnp1b*-tMO, 93% of embryos, n=27 for *adnp2b*-tMO and 67% of embryos, n=18 for *adnp2b*-spMP. *band3* 28 hpf: 86% of embryos, n=21 for *adnp1a*-sp$_1$MO, 79% of embryos, n=14 for *adnp1b*-tMO, 57% of embryos, n=38 for *adnp2b*-tMO and 95% of embryos, n=19 for *adnp2b*-

spMP. Embryonic *α-globin 1* 28 hpf: 100% of embryos, n=28 for *adnp1a*-sp$_1$MO, 86% of embryos, n=21 for *adnp1b*-tMO, 61% of embryos, n=28 for *adnp2b*-tMO and 74% of embryos, n=19 for *adnp2b*-spMP].

Figure S7.

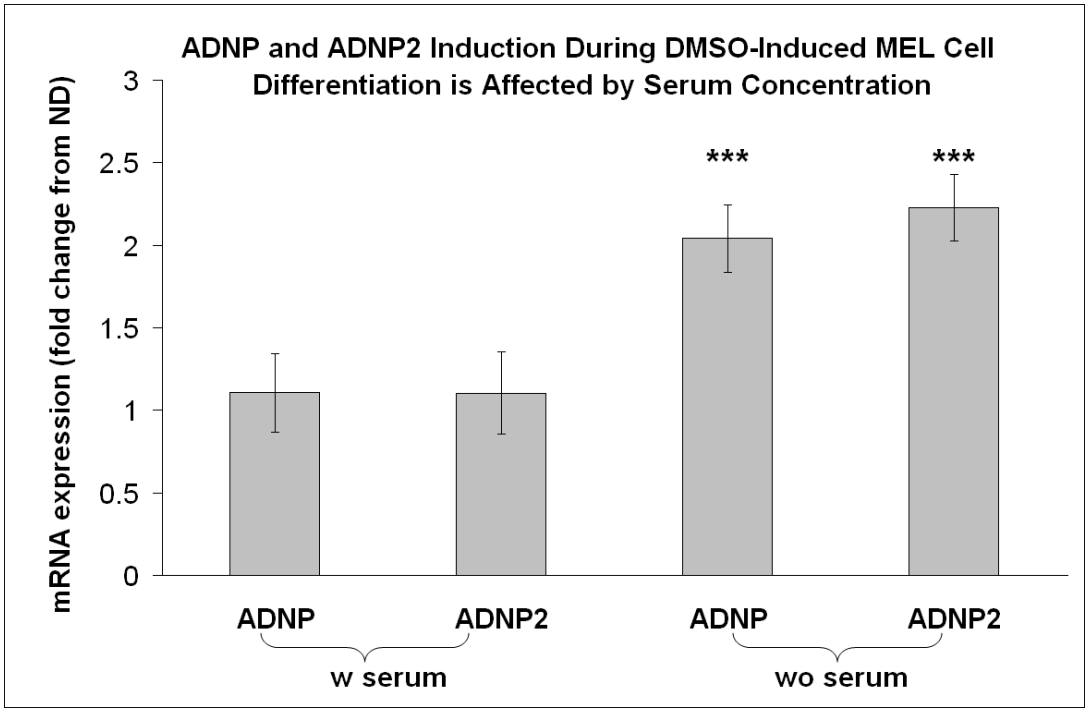

Figure S7. The effect of serum on the induction of ADNP and ADNP2 during DMSO-induced MEL cell differentiation. To study ADNP and ADNP2 mRNA expression during DMSO-induced MEL cell differentiation, cells were supplemented with 2% DMSO for 3-days, and the expression levels of ADNP and ADNP2 were evaluated in differentiated versus non-differentiated cells. Gene expression analysis indicated no significant change in the mRNA levels of ADNP and ADNP2 during MEL cell differentiation. Interestingly, 4-hours of culturing of the cells in the absence of serum (opti-MEM) before the addition of normal growth medium supplemented with 2% DMSO for 3-days (so

that the ratio between serum-free medium and normal medium was 3:5, respectively) up-regulated ADNP and ADNP2 levels in the DMSO-treated cells by 2-fold. Results were repeated 6-times with the addition of serum and 3-times in the reduced serum conditions, each in duplicate. Results, means ± S.E.M, are presented as fold-change from the expression in the non-differentiated state (ND). Statistical analysis included student's t-test (***p<0.001, relative to ND). Culturing cells in serum-free medium was shown before to affect proliferation, differentiation and gene expression both in MEL cells (14,15) as well as other cells (16,17).

Figure S8.

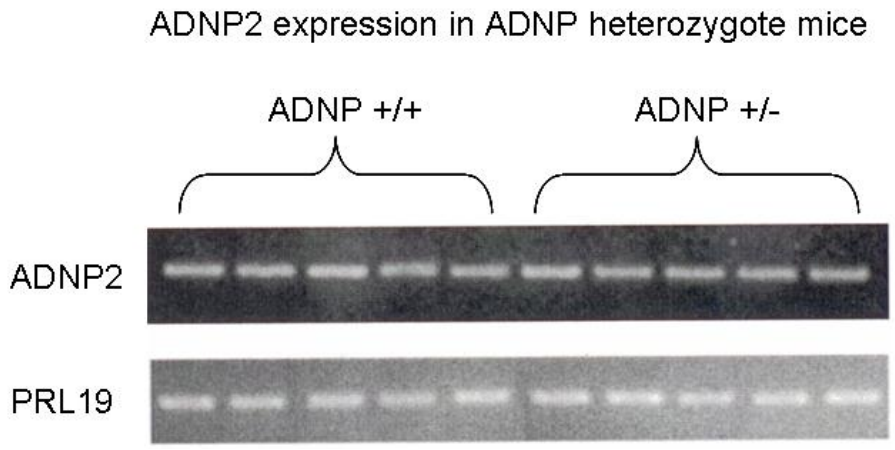

Figure S8. ADNP2 expression is constant in ADNP +/+ versus ADNP +/- mice. To study the effect of ADNP haploinsufficiency on the expression of its homolog gene ADNP2, RNA was extracted from brains (cortex) of 2 months old ADNP +/+ and ADNP +/- mice (5 mice in each group). PCR analysis was performed with PRL19 as the internal standard. No change in ADNP2 expression was observed between the groups (courtesy of Michal Kusnir, M.Sc. Thesis, Tel Aviv University).

The specificity of the RNA interference sequences was also ascertained in the P19 cell-line, demonstrating a 30% (p<0.001) or 45% (p<0.01) reduction in ADNP2 versus 7% (p=0.13) or 3% (p=0.44) reduction in ADNP, 24hrs or 48hrs after treatment with ADNP2 siRNA, respectively. Silencing of ADNP in these cells resulted in a 40% decrease in ADNP levels after 24hrs (p<0.05), and an insignificant 5% increase in ADNP2 levels (p=0.13). These observations essentially exclude mistargeting of the corresponding paralogue RNA, by showing no reciprocal regulation between ADNP and ADNP2.

Figure S9.

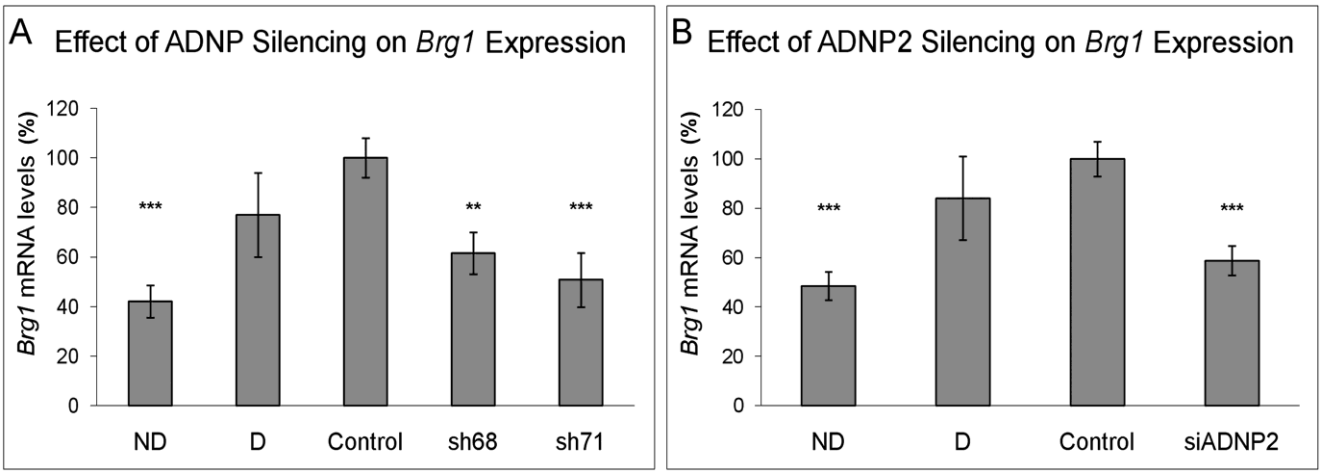

Figure S9. Impaired MEL cell differentiation as a result of ADNP/ADNP2 silencing is associated with reduced mRNA expression of the chromatin-remodeling protein *Brg1*. *Brg1* mRNA levels were evaluated by real-time PCR in samples from the ADNP (A) and ADNP2 (B) knockdown experiments. Results, means ± S.E.M (n=4 for ADNP and n=5 for ADNP2, each in triplicate) are presented as % from *Brg1* levels in control cells (transfected with non-specific shRNA/siRNA). One way ANOVA was performed to compare between the groups with post hoc Tukey HSD (**p<0.01, *** p<0.001, in comparison to control cells). ND= non-differentiated, D= differentiated. Results

demonstrated that *Brg1* RNA levels in non-differentiated MEL cells were ~2 times lower than the levels in differentiated cells, implying that *Brg1* was associated with erythroid differentiation in these cells. In ADNP and ADNP2 knockdown cells, *Brg1* levels were 40-50% lower than those in control cells treated with non-specific shRNA/siRNA sequences, similar to the levels in the non-differentiated cells. To ascertain changes at the protein level, western analysis for *Brg1* was performed however the results were variable and inconclusive, indicative of insignificant changes. The variability in the western results may be attributed to a complex mechanism of regulation of the key regulatory gene *Brg1*, as well as to differences in the efficacy of translation versus transcription (18). Interestingly, previous data suggested that *Brg1* protein expression was not significantly changed following MEL cell differentiation (19) in agreement with our results.

Figure S10

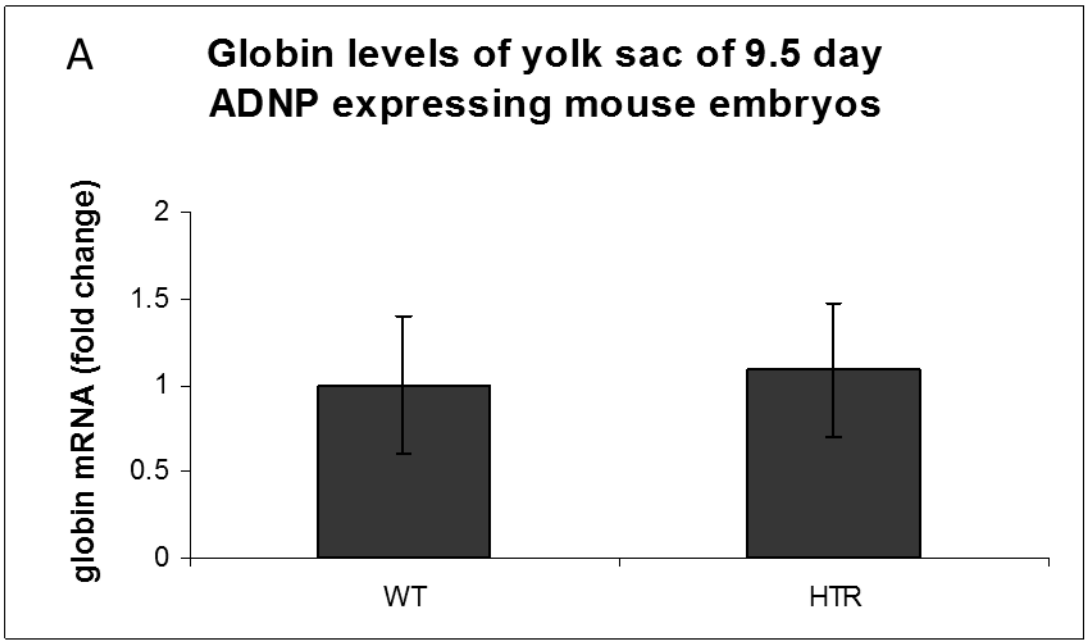

B	No.	Male to Female ratio	RBC	Hemoglobin
Wild-type	11	7:4	7.51±0.96 × 10^6/µl	11.6±1.18 g/dl
ADNP heterozygous	10	5:5	7.17±1.61 × 10^6/µl	11.16±2.38 g/dl

Figure S10A: The embryonic yolk sac of ADNP+/- (haploinsufficient) embryos exhibits similar amounts of *β-globin* mRNA as the yold sacs of intact ADNP+/+ embryos. Mice were maintained and experiments performed according to the guidelines for the care and use of laboratory animals of Tel-Aviv University, under Governmental permission. Experiments were conducted ADNP+/- female mice, subjected to breeding with ADNP+/- male mice, plug day was assigned as day 0 (E0). On day 9.5 (E9.5) whole embryos were separated from the extra embryonic tissue (yolk sac and amnion). The extra embryonic tissues were frozen in liquid nitrogen, and stored at − 80 °C until analysis, while the embryos were stored separately and used for genotyping (Transnetyx, Inc., Memphis, Tennessee,

USA), (20). RNA was isolated from each extra embryonic tissue (~90 mg) using the Qiagene RNeasy mini kit (Qiagene, Hilden, Germany). The amounts of RNA extracted from one tissue at age E9.5 was ~ 1 μg (n=5, ADNP+/- = heterozygous = HTR, and n=5 ADNP+/+ termed wild type = WT). *Beta-globin* mRNA levels were evaluated using Quantitative real-time PCR (see Table S2 for primers and reference 4 for protocol). Two independent experiments were performed, each in triplicates. Results are means ± S.E.M and presented as percentage from WT levels. Statistical analysis including student's t-test (Student's t-test), showed no difference between the experimental groups. An embryonic yolk sac from a knockout embryo tested side by side did not show a significant difference.

Figure S10B. Adult ADNP heterozygous mice (ADNP+/-) do not suffer from reduced hemoglobin levels. The effect of ADNP knockdown was further evaluated on adult ADNP heterozygous (ADNP+/-) mice. Blood was collected from 11 wild-type (7 males, 4 females) and 10 ADNP heterozygous (5 males, 5 females) 18-months-old mice (20). Animals were sacrificed and their blood was collected into blood collection tubes with EDTA. Analyses for complete blood counts were performed by the AML Veterinary Division at Herzliya Medical Center, Israel. Several parameters were measured including red blood cell (RBC) count, hemoglobin (Hb), hematocrit, mean corpuscular volume (MCV), mean corpuscular hemoglobin (MCH), mean corpuscular hemoglobin concentration (MCHC), white blood cell and platelets count. No significant differences in RBC count (p=0.28) or hemoglobin levels (p=0.3) were observed. Additional analysis was conducted on female and male groups separately, however no changes in RBC count or hemoglobin levels were noticed (data not shown). The other parameters were also similar between wild-type and heterozygous animals (data not shown).

Supplemental Movies (Legends and Still Images)

Movie S1.

Movie S1. Blood circulation in 48 hpf wild-type embryo versus *adnp2a*-tMO injected embryo. 48 hpf wild-type embryo (top) and *adnp2a*-tMO injected embryo (bottom). Red blood circulating the heart and blood vessels is visible in wild-type embryo, but not in *adnp2a*-tMO injected embryo.

Movie S2.

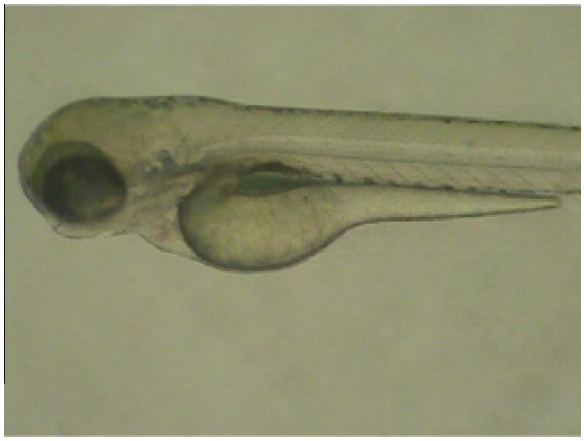

Movie S2. Blood circulation in 72 hpf wild-type embryo. 72 hpf wild-type embryo with red blood circulates in its heart and blood vessels.

Movie S3.

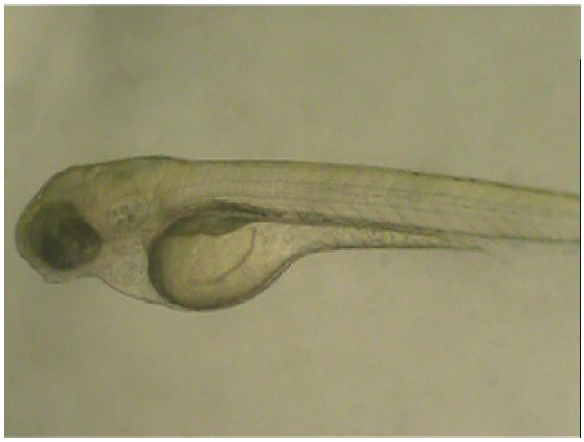

Movie S3. Blood circulation in 72 hpf *adnp2a*-tMO injected embryo.72 hpf *adnp2a*-tMO injected embryo with no blood in its heart and blood vessels. Cardiac edema is visible.

Movie S4.

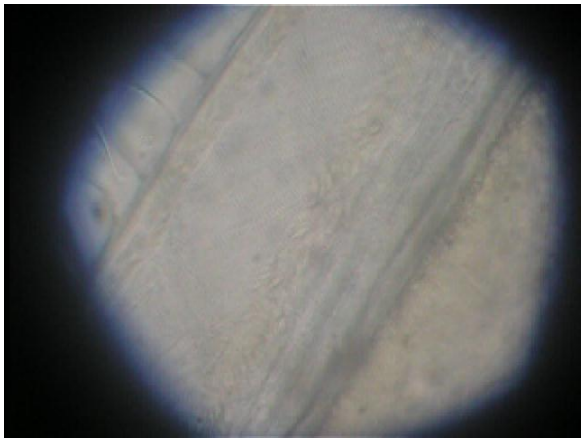

Movie S4. Blood circulation in 72 hpf wild-type embryo under light microscope. Many blood cells are circulating inside the blood vessels of 72 hpf wild-type embryo.

Movie S5.

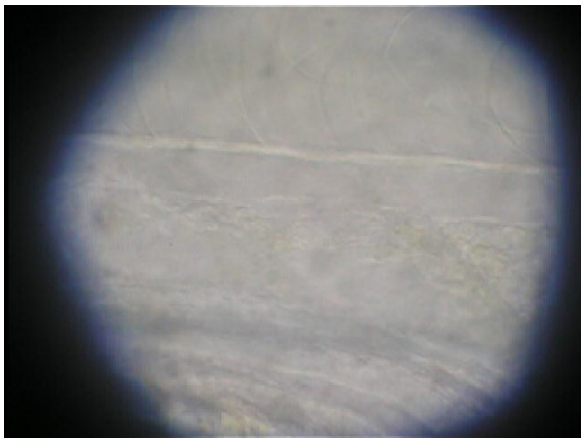

Movie S5. Blood circulation in 72 hpf *adnp2a*-tMO injected embryo under light microscope (1).

Only few blood cells are circulating inside the blood vessels of 72 hpf *adnp2a*-tMO injected embryo.

Movie S6.

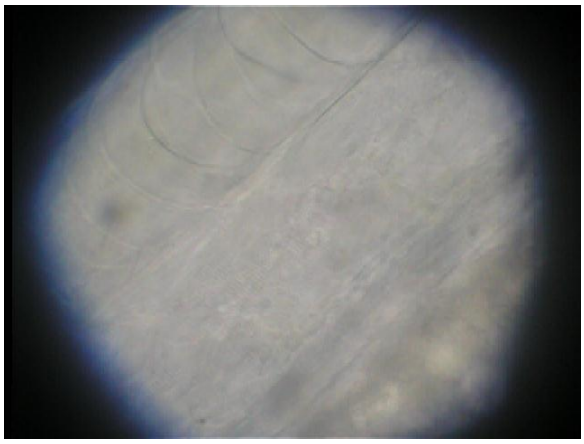

Movie S6. Blood circulation in 72 hpf *adnp2a*-tMO injected embryo under light microscope (2).

No blood cells are visible inside the blood vessels of another 72 hpf *adnp2a*-tMO injected embryo.

Supplemental References

1. Iuchi, I., and Yamamoto, M. (1983) Erythropoiesis in the developing rainbow trout, Salmo gairdneri irideus: histochemical and immunochemical detection of erythropoietic organs. *J Exp Zool* **226**, 409-417
2. Palevitch, O., Kight, K., Abraham, E., Wray, S., Zohar, Y., and Gothilf, Y. (2007) Ontogeny of the GnRH systems in zebrafish brain: in situ hybridization and promoter-reporter expression analyses in intact animals. *Cell Tissue Res* **327**, 313-322
3. Ziv, L., Levkovitz, S., Toyama, R., Falcon, J., and Gothilf, Y. (2005) Functional development of the zebrafish pineal gland: light-induced expression of period2 is required for onset of the circadian clock. *J Neuroendocrinol* **17**, 314-320
4. Dresner, E., Agam, G., and Gozes, I. (2010) Activity-dependent neuroprotective protein (ADNP) expression level is correlated with the expression of the sister protein ADNP2: Deregulation in schizophrenia. *Eur Neuropsychopharmacol*
5. Cocquet, J., Chong, A., Zhang, G., and Veitia, R. A. (2006) Reverse transcriptase template switching and false alternative transcripts. *Genomics* **88**, 127-131
6. Kozak, M. (1986) Point mutations define a sequence flanking the AUG initiator codon that modulates translation by eukaryotic ribosomes. *Cell* **44**, 283-292
7. Nasevicius, A., and Ekker, S. C. (2000) Effective targeted gene 'knockdown' in zebrafish. *Nat Genet* **26**, 216-220
8. Amores, A., Force, A., Yan, Y. L., Joly, L., Amemiya, C., Fritz, A., Ho, R. K., Langeland, J., Prince, V., Wang, Y. L., Westerfield, M., Ekker, M., and Postlethwait, J. H. (1998) Zebrafish hox clusters and vertebrate genome evolution. *Science* **282**, 1711-1714

9. Kane, D. A., and Kimmel, C. B. (1993) The zebrafish midblastula transition. *Development* **119**, 447-456

10. Itoh, M., Kudoh, T., Dedekian, M., Kim, C. H., and Chitnis, A. B. (2002) A role for iro1 and iro7 in the establishment of an anteroposterior compartment of the ectoderm adjacent to the midbrain-hindbrain boundary. *Development* **129**, 2317-2327

11. Thompson, M. A., Ransom, D. G., Pratt, S. J., MacLennan, H., Kieran, M. W., Detrich, H. W., 3rd, Vail, B., Huber, T. L., Paw, B., Brownlie, A. J., Oates, A. C., Fritz, A., Gates, M. A., Amores, A., Bahary, N., Talbot, W. S., Her, H., Beier, D. R., Postlethwait, J. H., and Zon, L. I. (1998) The cloche and spadetail genes differentially affect hematopoiesis and vasculogenesis. *Dev Biol* **197**, 248-269

12. Willett, C. E., Kawasaki, H., Amemiya, C. T., Lin, S., and Steiner, L. A. (2001) Ikaros expression as a marker for lymphoid progenitors during zebrafish development. *Dev Dyn* **222**, 694-698

13. Yelon, D., Horne, S. A., and Stainier, D. Y. (1999) Restricted expression of cardiac myosin genes reveals regulated aspects of heart tube assembly in zebrafish. *Dev Biol* **214**, 23-37

14. Pessano, S., McNab, A., and Rovera, G. (1981) Growth and differentiation of human and murine erythroleukemia cell lines in serum-free synthetic medium. *Cancer Res* **41**, 3592-3596

15. Ahearn, G. S., Daehler, C. C., and Majumdar, S. K. (1992) Serum-free media for murine erythroleukemia cells still not as good as serum-supplemented media. *In Vitro Cell Dev Biol* **28A**, 227-232

16. Mandl, E. W., Jahr, H., Koevoet, J. L., van Leeuwen, J. P., Weinans, H., Verhaar, J. A., and van Osch, G. J. (2004) Fibroblast growth factor-2 in serum-free medium is a potent mitogen

and reduces dedifferentiation of human ear chondrocytes in monolayer culture. *Matrix Biol* **23**, 231-241

17. Li, W. C., Ralphs, K. L., Slack, J. M., and Tosh, D. (2007) Keratinocyte serum-free medium maintains long-term liver gene expression and function in cultured rat hepatocytes by preventing the loss of liver-enriched transcription factors. *Int J Biochem Cell Biol* **39**, 541-554
18. Ghazalpour, A., Bennett, B., Petyuk, V. A., Orozco, L., Hagopian, R., Mungrue, I. N., Farber, C. R., Sinsheimer, J., Kang, H. M., Furlotte, N., Park, C. C., Wen, P. Z., Brewer, H., Weitz, K., Camp, D. G., 2nd, Pan, C., Yordanova, R., Neuhaus, I., Tilford, C., Siemers, N., Gargalovic, P., Eskin, E., Kirchgessner, T., Smith, D. J., Smith, R. D., and Lusis, A. J. (2011) Comparative analysis of proteome and transcriptome variation in mouse. *PLoS Genet* **7**, e1001393
19. Xu, Z., Meng, X., Cai, Y., Koury, M. J., and Brandt, S. J. (2006) Recruitment of the SWI/SNF protein Brg1 by a multiprotein complex effects transcriptional repression in murine erythroid progenitors. *Biochem J* **399**, 297-304
20. Vulih-Shultzman, I., Pinhasov, A., Mandel, S., Grigoriadis, N., Touloumi, O., Pittel, Z., and Gozes, I. (2007) Activity-dependent neuroprotective protein snippet NAP reduces tau hyperphosphorylation and enhances learning in a novel transgenic mouse model. *J Pharmacol Exp Ther* **323**, 438-449